Design and Field Evaluation of a Robotic Cotton Harvester with Improved Structural Balance and Suction Mechanism

Van Patiluna[1], Joe Mari Maja[1], Aashish Karki[2] and Edward Barnes[3]
[1]*Center of Applied Artificial Intelligence for Sustainable Agriculture, South Carolina State University, 300 College St, Orangeburg, SC, U.S.A.*
[2]*Department of Plant and Environmental Sciences, 171 Poole Agricultural Center, Clemson, SC, U.S.A.*
[3]*Cotton Incorporated, 6399 Weston Parkway, Cary, NC 27513, U.S.A.*

Keywords: Cotton Harvester, Robotics, Simulation.

Abstract: Mechanization in the cotton industry increased efficiency and productivity by reducing reliance on manual labor and improving overall output. Automation and robotics have been increasingly integrated into cotton production in the United States to address various challenges and enhance agricultural efficiency. Using robotics and automation in agriculture is a widespread idea whose technical feasibility has already been proven in several studies. The objective of this study is to design and implement a new robotic cotton harvester addressing the problems encountered with the previous design. It featured a redesigned finger roller and an optimized chassis to improve balance and structural integrity. The new design utilizes the same Amiga robotic platform that is capable of heavy loads such as the header assembly and power generators. A field experiment assessed harvesting efficiency under three different duty cycles corresponding to the speed of front finger rollers. During the experiment, the new design experienced clogging of the eductor inlet hindering the movement of cotton bolls to the collecting bin, which reduced harvesting efficiency. Although the harvesting efficiency was lower than ideal, it was still slightly better than the previous design. Adjusting the speed of the front finger rollers has no significant effect on the boll and trash collected, suggesting that lower speeds are ideal. The static stress simulation of the chassis revealed a better balance and structural integrity than the previous design. Overall, the new design of the cotton harvesting robot had better structural integrity, however, it requires further improvements to address clogging of the eductor inlet to move the fibers from the header assembly to the collecting bin, minimize the trash content and improve harvesting efficiency.

1 INTRODUCTION

Mechanization in the cotton industry has brought both significant benefits and challenges by increasing productivity by reducing reliance on manual labor but also raised concerns about labor displacement and the impact on traditional harvesting practices (Peterson & Kislev, 1986). The adoption of machine harvesting was driven largely by increased nonfarm wages and the declining cost of mechanized harvesting, reflecting the interplay between economic incentives and technological advancements (Peterson & Kislev, 1986). This transition reshaped labor markets in cotton-producing regions, with many traditional cotton pickers shifting to other sectors such as manufacturing (Jung, 2018).

Despite these economic gains, mechanization has also raised environmental and sustainability concerns. Cotton cultivation places considerable pressure on natural resources such as land and water, contributing to issues like soil degradation and the overuse of pesticides (Natálio & Maria, 2018).

In response to these challenges, automation and robotics have been increasingly integrated into U.S. cotton production to enhance efficiency and sustainability (Barnes et al., 2021). Recent advancements in precision agriculture, improved irrigation systems, and novel cotton varieties have enabled the development of autonomous multi-purpose robotic platforms (Maja et al., 2021). These platforms streamline operations, optimize resource use, and reduce the need for chemical inputs.

Currently, most cotton in the U.S. is harvested using large, heavy mechanical pickers (EPA, 2025). The weight of these machines causes soil compaction, which reduces long-term soil productivity (Al-Shatib

Patiluna, V., Maja, J. M., Karki, A. and Barnes, E.
Design and Field Evaluation of a Robotic Cotton Harvester with Improved Structural Balance and Suction Mechanism.
DOI: 10.5220/0013945700003982

In *Proceedings of the 22nd International Conference on Informatics in Control, Automation and Robotics (ICINCO 2025) - Volume 2*, pages 647-654
ISBN: 978-989-758-770-2; ISSN: 2184-2809

et al., 2021; Lagnelov et al., 2023; Antille et al., 2016). Furthermore, the high cost of such equipment requires large-scale operations of 600 to 800 hectares to justify a single machine (Barnes et al., 2021).

Several robotic cotton harvesting systems have been proposed to address these limitations. Examples include a wet/dry vacuum cleaner-based harvester (Fue et al., 2021), a Cartesian manipulator with a suction-based end-effector (Maja et al., 2021), and a three-fingered robotic end-effector using a pin tape mechanism (Gharakhani et al., 2022). A notable recent approach involves finger roller-based pickers, which collect bolls in bulk rather than individually, as demonstrated by Mail et al. (2023) at Clemson University. This method forms the foundation for the improved robotic harvester developed in this study.

The objective of this study is to design, build, and evaluate an improved robotic cotton harvester that addresses the mechanical limitations and performance issues identified in the previous prototype. A new prototype was developed, incorporating a redesigned finger roller and an optimized chassis, and was evaluated through static stress simulations and field experiments.

2 MATERIALS AND METHODS

2.1 Harvester Design

A new cotton harvester prototype was designed based on the findings from the previous prototype built. It maintained the same mechanism for collecting the cotton bolls that is using finger rollers to pluck the cotton bolls and an eductor system to move the bolls to the collecting bin. It also used the same robotic platform Amiga developed by Farm-NG (Watsonville, CA, USA) as shown in Figure 1.

Instead of using belts and pulleys to drive the finger rollers, an angled gearbox was used with 1:1 gear ratio used for the front rollers and 1:2 for the rear rollers. To produce the vacuum at the eductor, an 800 CFM leaf blower was utilized. A third blower was added to create to positive air pressure to blow the cotton bolls accumulating in the eductor inlet.

Figure 1: Amiga robotic platform with bare chassis.

Two 2200-Watt generators were used to power the blowers, motors and electronics system of the harvester. The Amiga platform was powered by its own battery pack. Figure 2 shows the sketch of the previous design (a) and new design (b).

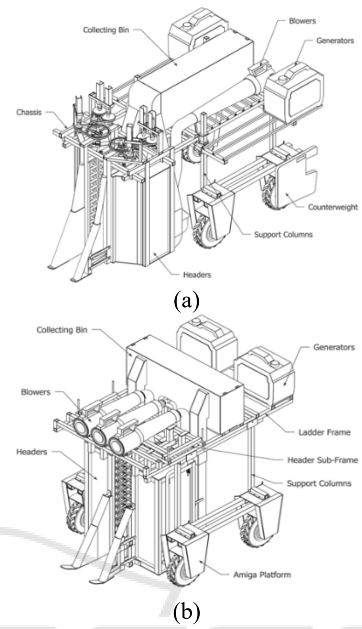

Figure 2: Sketches of the previous design (a) and the new design (b).

The rollers were driven by a 100 rpm and 320 rpm planetary gear motors for the front and rear rollers respectively. The speed of the front rollers can be adjusted to three duty cycles: 25%, 50% and 100%. The shaft speed of the rear rollers was fixed at 320 rpm enough to pluck the cotton bolls from the fruiting branch. Powering the motors were 2x15A and 2x30A RoboClaw (BasicMicro, Temecula, CA, USA) motor controllers. The configuration of the front finger roller was modified as shown in Figure 3. In the previous design, the front and rear rollers were offset at an angle of about 54 degrees (Figure 3a). In the revised design, the rollers are aligned side-by-side (Figure 3b).

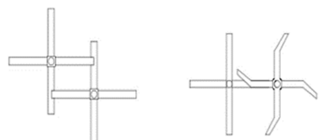

(a) (b)

Figure 3: Finger roller orientation of the previous design (a) and new design (b).

The offset in the original design aimed to narrow the header but reduced the rear roller's effectiveness, since it only hit cotton bolls pulled deep enough by the front roller. By aligning the rollers side-by-side, cotton bolls do not have to be pulled deep enough to be reached by the rear finger rollers (Maja et. al., 2024). The fingers were made of aluminum, laser cut to have 15-degree bend (Figure 3b).

The new design also focused on improving the structural integrity of the robot chassis, addressing the observed stresses and displacements from the field trials of the previous design. Structural improvements were introduced. First, ground clearance could be adjusted through a separate sub-frame (Figure 2b). It can be raised to adjust the ground clearance up to a maximum travel of 100 mm. Secondly, the balance of the entire robot can be adjusted by sliding the ladder frame front or back. All the robots' components including the headers, ducts, collecting bin, blowers, electronics and generators were mounted on the ladder frame. This free movement of the ladder frame allows the load to be moved along the support columns to adjust the balance and weight distribution as needed. A third blower was added to produce positive air pressure to clear out stuck cotton bolls and trash on the eductor inlet. The new design widened the chassis by 4.3% to 1.62 m, while maintaining a wheelbase of 0.96 m. Figure 4 shows the completed robot.

(a) (b)

Figure 4: Front (a) and rear (b) views of the completed assembly of the robotic cotton harvester.

Table 1: Weights of the load components.

Component	Previous	New
Header gross weight	75.47 kg	85.79 kg
Generator dry weight	24.99 kg (245.06 N)	

Static-stress simulation of the chassis of the previous and new design was conducted to evaluate the structural integrity of the chassis using Autodesk Fusion (Autodesk, San Francisco, CA, USA). Simulated loads of the heavy components such as the header assembly and power generators were applied to the chassis (see Table 1). Mechanical properties of the materials used of the construction of the chassis such as AISI 1018 and Aluminum 6061 (header assembly) and 5052 H32 (chassis) were used applied in the materials properties for simulation. Load was also applied to the header assembly equivalent to the bending force of a cotton stalk, about 63.64 N (Khudayarov et. al., 2022; Zao et. al., 2022).

The load setup will provide the ultimate loads test for the chassis. Once simulations were completed, key parameters such as von Mises stress, displacement, strain and safety factors were analyzed using visualization tools and quantitative metrics provided by the simulation software (Jahanbakhshi et.al., 2019).

2.2 Control System

A MikroE Clicker 4 for STM32F (Belgrade, Serbia) microcontroller board was used to control the motors, blowers and handles wireless communication with the base computer. Attached to the Clicker 4 board were UART MUX 4 Click (to handle serial communication with the motor controllers), Relay 5 Click (to control the AC power to the blowers) and XBee 3 Click (for wireless communication). Figure 5 shows the block diagram of the control system.

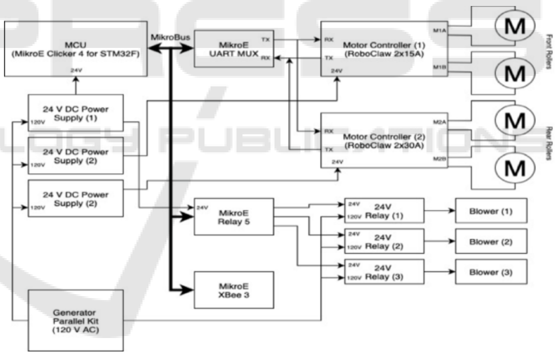

Figure 5: Control system block diagram.

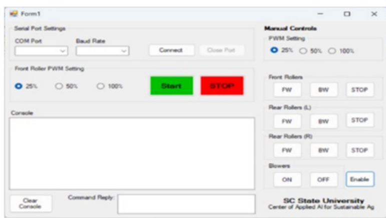

Figure 6: Dashboard and control software.

Three 24V DC power supply powered the microcontroller and motor controllers. These power supplies were also powered by a 120V AC coming from the combined output the two generators through a parallel kit. A dashboard software was developed to control the system remotely (Figure 6). It featured an automatic startup sequence (start button) and system-wide shut down (stop button).

An automatic startup sequence was implemented to manage the proper activation order of the motors and blowers, thereby preventing power surges caused by simultaneous current draw. The startup configuration also enables pre-selection of the front roller speed, which can be set to 25%, 50%, or 100% duty cycle—corresponding to approximate shaft speeds of 25 rpm, 50 rpm, and 100 rpm, respectively. In addition to the automated sequence, the dashboard software provides manual control options. An XBee transceiver connected to the base computer facilitates wireless communication with the controller module.

2.3 Study Site

The experiment and data collection were conducted at the South Carolina State University Research and Demonstration Farm in Olar, SC, USA (33.162161, -81.136361). The cotton variety used was Deltapine DP 2127 B3XF. The field was planted in a 1:1 skip-row configuration to accommodate the robotic harvester and to provide maneuvering space for the research crew. Figure 7 shows an aerial view of the cotton field used for the experiment.

Figure 7: Aerial shot of the cotton farm at SC State Research and Demonstration farm.

Due to planting delays, cotton was sown on June 14, 2024. Chemical defoliants were applied on November 27, 2024, and the harvesting experiments were conducted approximately one month later, on December 23, 2024.

The experimental design followed a completely randomized design (CRD) with three (3) treatments and three (3) replications per treatment. The objective was to evaluate the effect of front finger roller speed on the number of cotton bolls and the amount of trash collected during harvesting. Details of each treatment are provided in Table 2.

Table 2: Experiment Treatment Details.

Treatment A	Front finger rollers at 50% duty cycle.
Treatment B	Front finger rollers at 25% duty cycle.
Treatment C	Front finger rollers at 100% duty cycle.

A total of nine rows were selected and prepared for the study. Each row measured 3 meters in length, with a minimum buffer zone of 1.5 meters between rows to prevent cross-contamination and allow robot maneuverability. The layout and locations of the treatment rows are shown in Figure 8. To minimize the time and effort required to reposition the robot between rows, an optimized experimental sequence was developed.

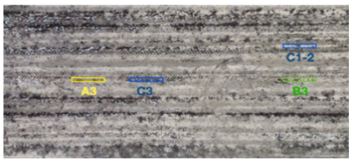

(a)

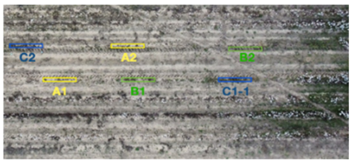

(b)

Figure 8: Selected treatment rows with buffer zones: (a) Treatments A3, C3, B3 and C1; (b) Treatments A1, A2, B1, B2 and C2. C1-1 was replaced by C1-2 as treatment C1.

Instead of running treatments in a strict numerical order, the robot followed a path that allowed for the most efficient traversal across the field. The sequence was as follows: A1-B1-C1-B2-A2-C2-B3-C3-A3.

The robot was configured with the appropriate duty cycle setting for the front finger rollers, based on the treatment assignment. The startup sequence was executed using the developed dashboard software to ensure that the motors for both the front and rear rollers started in the correct order. The robot was positioned at the center of the selected row (Figure 9) and driven forward at a constant speed of approximately 0.2 m/s.

Figure 9: Harvester robot positioned to harvest cotton bolls from the treatment row.

Cotton bolls were collected from four distinct locations: (1) inside the collecting bin, (2) within the eductor duct, (3) on the ground, and (4) remaining unharvested on the plant. The collected bolls were placed into separate, labeled paper bags for each treatment. After the experiment, cotton fibers were separated from foreign materials such as leaves and stalk fragments that were inadvertently collected during harvesting. The cleaned cotton fiber and associated trash were then weighed separately.

Due to the mechanical damage inflicted by the harvesting process, most bolls were too mangled to be counted individually. To estimate the number of cotton bolls collected from each source (bin, header, ground, and plant), the total fiber weight was divided by 5.3 grams—the average weight of a single Deltapine DP 2127 B3XF cotton boll. The average boll weight was determined by sampling and weighing intact bolls from the same experimental field. After the number of cotton bolls were determined, the harvesting efficiency of the robotic cotton harvester was calculated using Equation (1).

$$efficiency = \frac{output}{input} x100\% \quad (1)$$

where:

output – number bolls collected in the bin
input – total number of cotton bolls collected

The input data included the estimated number of cotton bolls collected from four locations: the collecting bin, header assembly, ground, and remaining on the plant. Trash content, consisting primarily of leaves, stems, and other debris, were quantified by its weight relative to the total harvested material.

To calculate the percentage of trash collected in the bin and header assemblies, Equation (2) below was used.

$$\%\, trash = \frac{trash\ weight}{trash + fiber\ weight} x100\% \quad (2)$$

Trash found on the ground and on the plant were excluded from analysis, as it was not mechanically collected during the experiment and therefore not attributable to the harvester's performance.

3 RESULTS

3.1 Static Stress Analysis of the Chassis

After the simulation, the results revealed a concentration of stress in the cantilever structure of the previous design (Figure 10b). In contrast, the new design exhibited moderate stress localized on one of the crossbars of the header sub-frame (Figure 10a).

The elevated stress observed in the previous design was attributed to the header assembly being supported solely by the front columns of the chassis, creating a cantilevered overhang effect.

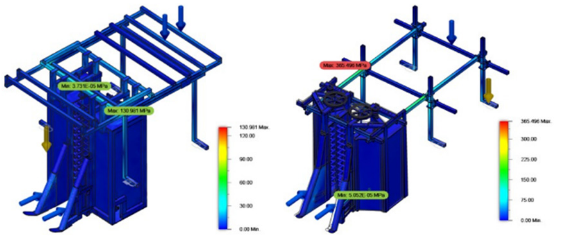

(a) (b)

Figure 10: Stress visualization of the integrated stress analysis for the (a) previous design and (b) new design showing von Mises stress.

In the redesigned system, the headers were supported on all four sides, allowing the load to be distributed more evenly across the sub-frame. Quantitative simulation data comparing the two designs is summarized in Table 3.

Table 3a: Static stress simulation data for the previous design.

Data	Min	Max
Stress (von Mises)	5.025E-05 MPa	365.496 MPa
Displacement	0.00 mm	49.383 mm
Strain	4.240E-10	0.003
Safety Factor	0.566	15.00

Table 3b: Static stress simulation data for the new design.

Data	Min	Max
Stress (von Mises)	3.731E-05 MPa	130.981 MPa
Displacement	0.00 mm	3.223 mm
Strain	1.938E-10	0.001
Safety Factor	1.58	15.00

The previous design exhibited a significantly higher von Mises stress of 365.496 MPa, compared to 130.981 MPa observed in the new design. In the previous design, stress was primarily concentrated at the frame joints between the cantilever and the support columns. Both designs experienced strain in the same high-stress regions, with the previous design showing a peak strain of 0.003, while the new design showed a lower value of 0.001. As expected, the maximum displacement was also greater in the previous design, measured at 49.38 mm at the stalk lifter. The simulation did not fully account for dynamic displacement in the cantilever structure, but further inspection of the integrated model revealed a pronounced increase in displacement at the cantilever section, as illustrated in Figure 11.

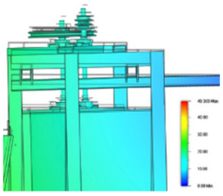

Figure 11: Displacement of the chassis of the previous design.

The high stress concentration observed in the previous design resulted in a safety factor of only 0.57, indicating a high risk of permanent deformation or even material failure under operational loads. This value fell below both the yield and ultimate tensile strengths of the material, suggesting structural inadequacy. In contrast, the new design achieved a 64.18% reduction in von Mises stress compared to the previous version and exhibited substantially lower displacement with no bending or deformation.

3.2 Cotton Boll Harvesting

After weighing the collected cotton fibers, the approximate number of cotton bolls from each collection point—the collecting bin, inside the headers, on the ground, and remaining on the plant—was estimated by dividing the fiber weight by the average weight of a single boll (5.3 grams).The estimated distribution of cotton bolls across these collection points is illustrated in Figure 12.

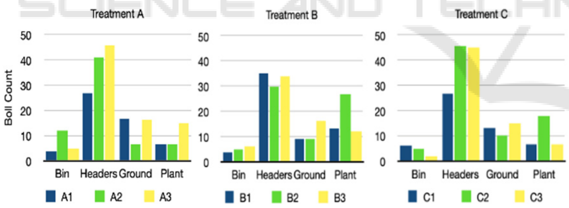

(a) (b) (c)

Figure 12: Cotton boll count collected from the bin, headers, ground and plant from (a) Treatment A, (b) Treatment B, and (c) Treatment C.

The data revealed that most cotton bolls were collected from within the header assembly (near the eductor inlet), while the smallest quantity was recovered from the collecting bin. This indicated that many bolls were unable to move from the header to the bin, suggesting a failure in the boll transfer process. Upon inspection, it was confirmed that cotton bolls and plant debris had clogged the eductor inlet (Figure 13), thereby restricting the vacuum airflow needed to move the material.

Figure 13: Cotton bolls and trash accumulating on the eductor inlet.

This blockage was likely exacerbated by the long delay between defoliation and harvesting, during which colder temperatures caused the plants to become brittle. Consequently, broken branches and stalk fragments accumulated at the inlet, further impeding airflow. The positive air pressure generated by the third blower, approximately 20 psi, was insufficient to effectively clear the obstruction. According to the spindle-type harvester in-season procedures (Cotton Inc.), it would take around 125 psi to effectively remove lint build up (cotton fiber) and trash. Among the treatments, Treatment A yielded the highest number of cotton bolls transferred to the collecting bin, while Treatment C had the highest accumulation within the header.

Due to the blocked/clogged eductor inlet, it was expected that the harvesting efficiency would be lower. Although some treatments like A2 and C1 have more than 10% harvesting efficiency, it was much lower than the ideal of 100%, as shown in Figure 14.

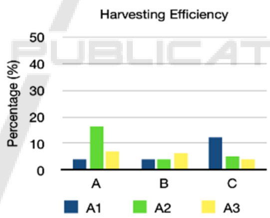

Figure 14: Harvesting efficiency for the 3 treatment rows.

The average for treatments A, B and C was 9.25%, 4.95% and 7.02% respectively. Treatment B had the lowest harvesting efficiency while treatment A had the highest. The previous design has an average harvesting efficiency of 5.77%, 5.72% and 8.1% for treatments A, B and C respectively. The new design has the highest efficiency at 9.25% for treatment A (50% duty cycle) while the previous has the highest efficiency at 8.1% for treatment C (100% duty cycle). The results revealed that the new design has the highest efficiency when the front finger roller is rotating at 50 rpm while the previous design achieved the highest efficiency at full speed of 100 rpm. Overall, the new design has slightly better results at 50% and 100% duty cycles compared to the previous.

The percentage of trash collected from the collecting bin, headers, ground and plants are shown in Figure 15. Treatment C has the least amount of trash at the collecting bin. It also has the most trash collected at the headers. Treatments A and B have below 50% trash in either collecting bin and headers. The data also shows that almost half of the weight collected in the collecting bin and headers were trash. The average trash percentage at the bin were 39.96%, 39.6% and 32.58% for treatments A, B and C respectively.

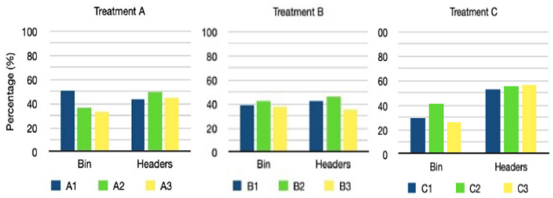

(a) (b) (c)

Figure 15: Percentage of trash collected from the collecting bin and headers among cotton fibers for Treatments A (a), B (b) and C (c).

Meanwhile, the average trash percentage from the headers were 46.28%, 41.35% and 55.08% for treatments A, B and C respectively. Unfortunately, the data from the previous design only weighed the branches wrapped around the finger rollers which excluded the twigs and leaves, therefore comparison to the current data could not be made.

The effect of the duty cycle applied to the motors of the front finger roller to the cotton bolls and trash collected was analyzed using one-way ANOVA. Table 4 shows the result of the analysis.

Table 4a: Effect of PWM applied to front finger rollers on number of bolls collected.

Treat	B_Bin	B_Head	B_Gnd	B_Plnt
A	5.23	32.50	9.95	15.11
B	3.31	27.19	9.33	15.59
C	3.13	0.19	10.82	6.74
F	0.7057342	0.6981467	0.1536920	0.6351503
p-value	0.5305679	0.5338403	0.8608073	0.5620781
F-Crit	5.1432529	5.1432529	5.1432529	5.1432529

Table 4b: Effect of PWM applied to front finger rollers on amount of trash collected.

Treat	T_Bin	T_Head	T_Gnd	T_Plnt
A	16.78	156.00	27.25	15.08
B	8.61	101.25	19.19	28.16
C	7.97	185.18	29.27	16.55
F	1.98574193	2.3709049	8.35233882	3.64021987
p-value	0.21785843	0.1742695	0.00757796	0.06389921

The results revealed no significant differences between different PWM duty cycles on the number of bolls collected in the bin (p=0.5305), headers (p=0.5338), ground (p=0.8608) and plant (p=0.5620) (Table 3a). This suggests that varying the shaft speed of the front finger rollers had minimal influence on the efficiency of harvesting. The amount of trash collected along with the cotton fibers in the collecting bin (p=0.2178) and headers (p=0.1742) were also non-significant (Table 3b), suggesting that the speed of front finger rollers did not change the trash amount. Thus, in this scenario, it would be ideal to operate at lower speeds to reduce energy use and lessen the wear and tear of the motors.

4 CONCLUSIONS

The new robotic cotton harvester was successfully designed, constructed, and tested in field conditions. All core systems functioned as intended, with only minimal operational issues. However, the field experiment revealed a critical limitation: a significant number of cotton bolls failed to reach the collecting bin due to blockage at the eductor inlet caused by accumulated trash and fiber. This obstruction reduced the effectiveness of the vacuum transfer system.

The third blower, intended to generate positive air pressure to clear the inlet, produced only about 20 psi, way insufficient to remove blockages during operation. As a result, most of the harvested bolls remained within the header, limiting overall harvesting efficiency. Although the new system performed slightly better than the previous version at 50% and 100% duty cycles, only a small fraction of the harvested bolls reached the collecting bin. Trash content remained high, accounting for at least 50% of the material collected in both the bin and header assemblies.

Analysis showed that varying the duty cycle of the front finger rollers (25%, 50%, 100%) had no significant effect on the number of cotton bolls collected or the amount of trash recovered. Therefore, operating the rollers at the lowest speed (25% duty cycle or 25 rpm) is recommended, as it reduces power consumption and mechanical wear without compromising performance.

The static stress simulation revealed a stark contrast between the two chassis designs. The previous version exhibited excessive von Mises stress at the cantilever structure—6.5 times higher than the acceptable limit—resulting in a safety factor below 1, indicating a high risk of permanent deformation or failure. In contrast, the new design demonstrated improved stress distribution, minimal displacement, and enhanced structural integrity under load. The optimized weight distribution also reduces the load on the front motors, lowering operating temperatures and extending motor lifespan.

While the new robotic harvester marks a substantial improvement in structural design and robustness, further enhancements are required to address boll transfer issues and trash reduction. If cotton bolls retained in the header were successfully transferred to the collecting bin, harvesting efficiency could increase by as much as 60%. Additionally, implementing strategies to minimize trash intake will be essential to improve fiber purity and overall performance.

ACKNOWLEDGEMENTS

The authors gratefully acknowledge Cotton Incorporated for funding this project under Project No. 24-061. Special thanks are extended to Ms. Melissa Mitchell and Dr. Lamin Drammeh of South Carolina State University 1890 Research & Extension for their continued support and guidance throughout the duration of this research.

REFERENCES

Antille, D. L.; Bennett, J. M. L.; Jensen, T. A. (2016) Soil compaction and controlled traffic considerations in Australian cotton-farming systems. *Crop Pasture Sci.*, *67*, 1–28. http://dx.doi.org/10.1071/CP15097

Barnes, E.; Morgan, G.; Hake, K.; Devine, J.; Kurtz, R.; Ibendahl, G.; Holt, G. (2021) Opportunities for Robotic Systems and Automation in Cotton Production. *Agriengineering*, *3*, 339–362. https://doi.org/10.3390/agriengineering3020023

Cotton Inc. (2025, September 11). The Spindle-Type Cotton Harvester In-Season Procedures https://www.cottoninc.com/cotton-production/ag-resources/harvest-systems/the-spindle-type-cotton-harvester/in-season-procedures.

EPA, U.S. Environmental Protection Agency. Available online: https://www3.epa.gov/ttn/chief/ap42/ch09/final/c9s03-1.pdf (accessed 12 July 2025).

Fue, K.; Porter, W.; Barnes, E.; Li, C. (2020) Rains, G. Center-articulated hydrostatic cotton harvesting rover using visual-servoing control and a finite state machine. *Electron*, *9*, 1–21. https://doi.org/10.3390/electronics9081226

Fue, K.; Porter, W.; Barnes, E.; Li, C.; Rains, G. (2020) Evaluation of a Stereo Vision System for Cotton Row Detection and Boll Location Estimation in Direct Sunlight. *Agronomy*, *10*, 1137. https://doi.org/10.3390/agronomy10081137

Gharakhani, H., Thomasson, J.A. Lu, Y. (2022) An end-effector for robotic cotton harvesting. *Smart Agricultural Technology*, Vol. 2. https://doi.org/10.1016/j.atech.2022.100043

Jahanbakhshi, A.; Heidarbeigi, K. (2019) Simulation and Mechanical Stress Analysis of the Lower Link Arm of a Tractor Using Finite Element Method. *Journal of Failure Analysis and Prevention*, 19, 1666–1672. https://doi.org/10.1007/s11668-019-00763-2

Jung, Y. (2018). The legacy of king cotton: agricultural patterns and the quality of structural change. *SocArXiv*. https://doi.org/10.31235/osf.io/trjfz

Khudayarov, B.M; Kuziev, U.T.; Sarimsakov, B.R.; Khuydaykulov, R.F. (2022) Dependence of the bending force on the morphology of cotton stems and on the parameters of the stalk bender. *IOP Conf. Ser.: Earth Environ. Sci.*, 1076 012045. https://doi.org/10.1088/1755-1315/1076/1/012045

Lagnelöv, O.; Larsson, G.; Larsolle, A.; Hansson, P. (2023) Impact of lowered vehicle weight of electric autonomous tractors in a systems perspective. *Smart Agricultural Technology*, 4, 100156. https://doi.org/10.1016/j.atech.2022.100156

Mail, M.F., Maja, J.M., Marshall, M., Patiluna, V., Cutulle, M., Miller, G., Bridges, W., Barnes, E. (2024) Development of New Cotton Harvesting Robot. *In 2024 Beltwide Cotton Conference, Fort Worth, TX, USA, 3-5 January 2024*, pp. 649-657.

Maja, J.M., Mail, M.F., Patiluna, V., Miller, G., Cutulle, Marshall, M., Barnes, E. (2024) A new mobile robot harvesting prototype for cotton production. *In AgEng 2024 Conference, Athens, Greece, 1-4 July 2024*, pp. 328-336.

Maja, J.; Polak, M.; Burce, M.; Barnes, E. (2021) CHAP: Cotton-Harvesting Autonomous Platform. *Agriengineering*, *3*, 199–217. https://doi.org/10.3390/agriengineering3020013

Natálio, F. and Maria, R. (2018). Structural evolution of gossypium hirsutum fibers grown under greenhouse and hydroponic conditions. *Fibers*, 6(1), 11. https://doi.org/10.3390/fib6010011

Peterson, Willis & Kislev, Yoav. (1986). The Cotton Harvester in Retrospect: Labor Displacement or Replacement? *The Journal of Economic History*, 46(1), 199-216.

Zhao, W.; Xie, J.; Wang, Z.; Gao, Q.; Chen, M. (2022) Investigation of mechanical properties of cotton stalk based on multi-component analyses. *Int. Agrophys.*, 36, 257-267. https://doi.org/10.31545/intagr/152488